Measurement of $R = \sigma_L/\sigma_T$
on Deuterium in the Nucleon Resonance Region

May 27, 2002

M.E. Christy (spokesperson), C. Keppel (spokesperson)
Hampton University, Hampton, VA

D. Gaskell, E. Kinney
University of Colorado, Boulder, Colorado

P. Markowitz, J. Reinhold
Florida International University, University Park, FL

I. Niculescu
James Madison University, Harrisonburg, VA

P. Bosted
University of Massachusetts, Amherst, MA

J. Dunne
Mississippi State University, Mississippi State, MS

A. Gasparian
North Carolina A&T State University, Greensboro, NC

R. Ent, M. Jones, D. Mack, S. Wood
Thomas Jefferson National Accelerator Facility, Newport News, Virginia, VA

H.P. Blok
Vrije Universiteit, Amsterdam, Netherlands

Abstract

We propose to measure the longitudinal-transverse (L-T) separated structure functions from deuterium throughout the nucleon resonance region ($1 < W^2 < 4$ GeV^2) and spanning the four-momentum transfer range $0.5 < Q^2 < 4.0$ (GeV/c)^2. The separation of the inclusive electroproduction cross sections into longitudinal and transverse strengths will accomplished by performing Rosenbluth separations to extract the transverse structure function $F_1(x, Q^2)$, the longitudinal structure function $F_L(x, Q^2)$, and the ratio $R = \sigma_L/\sigma_T$. This proposal represents the first global survey of these fundamental separated quantities in the resonance region.

The analysis of the separated resonance region proton data from experiment E94-110 [1], which was performed in Hall C, has recently been completed and the excellent precision obtained from that measurement will be presented here. The extension of the proton measurements to deuterium is straightforward and allows the precision of the proposed measurements to be predicted with great confidence. In addition, the analysis machinery which was developed for E94-110 can be used with only very little modification. The great care and time invested in developing the experimental requirements, systematic uncertainty measurements, and analysis machinery will be of immediate benefit to the proposed experiment.

1 Physics Overview

Due to the small value of the electromagnetic coupling constant, the scattering of electrons from nucleons can be well approximated by the exchange of a single virtual photon, which carries the exchanged 4-momentum squared, q^2. In terms of the incident electron energy, E, the scattered electron energy, $E^{'}$, and the scattering angle, θ, the absolute value of the exchanged 4-momentum squared is given by

$$(-q)^2 = Q^2 = 4EE^{'}\sin^2\frac{\theta}{2}. \tag{1}$$

In the one photon exchange approximation, the spin-independent cross section for inclusive electron-nucleon scattering can be expressed in terms of the photon helicity coupling as

$$\frac{d\sigma}{d\Omega dE^{'}} = \Gamma\left[\sigma_T(x, Q^2) + \epsilon\sigma_L(x, Q^2)\right], \tag{2}$$

where σ_T (σ_L) is the cross section for photo-absorption of purely transverse (longitudinal) polarized photons,

$$\Gamma = \frac{\alpha E^{'}(W^2 - M_p^2)}{2\pi Q^2 M_p E(1-\epsilon)} \tag{3}$$

is the flux of virtual photons, and

$$\epsilon = \left[1 + 2(1 + \frac{\nu^2}{Q^2})\tan^2\frac{\theta}{2}\right]^{-1} \tag{4}$$

is the polarization parameter for virtual photons.

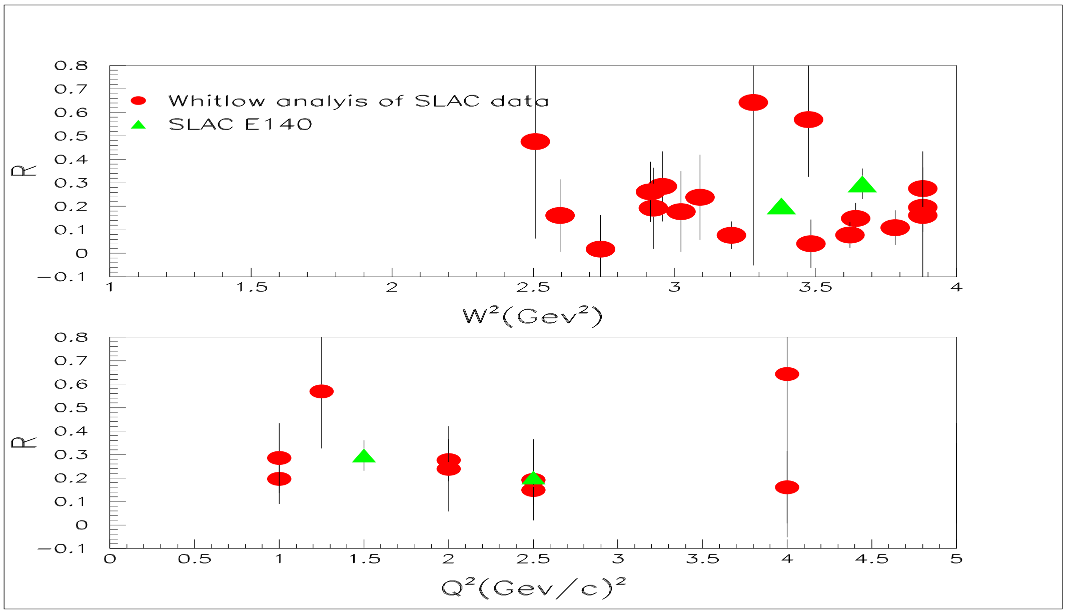

Figure 1: The world's data set of R on deuterium in the resonance region with W^2 (top) and Q^2 (bottom). The top panel includes measurements which extend to $Q^2 = 20$ (GeV/c)^2.

In terms of the structure functions $F_1(x,Q^2)$ and $F_2(x,Q^2)$, the double differential cross section can be written as

$$\frac{d\sigma}{d\Omega dE'} = \Gamma \frac{4\pi^2\alpha}{x(W^2 - M_p^2)} \left[2xF_1(x,Q^2) + \epsilon \left(\frac{1+4M_p^2x^2}{Q^2} F_2(x,Q^2) - 2xF_1(x,Q^2) \right) \right]. \tag{5}$$

Comparison of equations 2 and 5 shows that $F_1(x,Q^2)$ is purely transverse, while the combination

$$F_L(x,Q^2) = \frac{1+4M_p^2x^2}{Q^2} F_2(x,Q^2) - 2xF_1(x,Q^2) \tag{6}$$

is purely longitudinal. The separation of the unpolarized structure functions into longitudinal and transverse parts from cross section measurements can be accomplished via the Rosenbluth technique [9], by making measurements at two or more values of ϵ for fixed x and Q^2. Fitting the reduced cross section, $d\sigma/\Gamma$, linearly in ϵ, yields σ_T (and therefore $F_1(x,Q^2)$) as the intercept, and the structure function ratio $R(x,Q^2) = \sigma_L/\sigma_T = F_L(x,Q^2)/2xF_1(x,Q^2)$ as the slope.

2 Motivation and Goals

The existing world's resonance region measurements of R on deuterium from SLAC [10, 11, 12] are shown in Figure 1 as a function of both W^2 and Q^2. In this region the data is both sparse and of low quality, with typical errors on R of 100% or larger. In addition, there are no deuterium measurements of R below $W^2 < 2.5$ (GeV^2). This prevents any extraction of the separated structure functions from deuterium for the lower mass resonances. For the proton measurements, PAC 11 stated that "the L/T ratio on the proton is a fundamental quantity that should be measured with the best possible accuracy." This argument is no less true for the deuteron, the simplest nuclear system, or for the neutron. Neutron data will be obtained by subtracting the hydrogen E94-110 data from the proposed deuterium data.

The E94-110 proton R measurements allowed for the first precision tests of parton-hadron duality in all unpolarized structure functions. With this and the previous JLab Hall C measurements, duality has been shown to be a fundamental property of nucleon structure. This work has inspired renewed theory interest on the topic (see for example [2, 3, 4, 5, 6]), and the proposed data will add more valuable information. Specifically, Close and Isgur [7] argue that the neutron structure functions should exhibit "systematic deviations from local duality." In their approach, minimal necessary conditions are identified for duality to occur in a simple harmonic oscillator quark model and these conditions occur at higher W for the neutron than for the proton.

This experiment also addresses new calculations by Miller [8] predicting significant pion excess enhancement in the σ_L^A/σ_L^D ratio at low Q^2 and moderate x_{Bj}, as shown in figure 2. These kinematics fall within the proposed measurement, which will obtain both deuterium and aluminum target data (the latter for target background measurements, as outlined below). The question "Where are the nuclear pions?" has been an outstanding problem in nuclear physics for decades now. The belief that pions are the carrier of the nuclear force is a basic premise of nuclear physics. While this premise seemed verified by the original electromagnetic scattering (EMC effect) experiments, it was later brought into question by deep inelastic Drell-Yan lepton-nucleus measurements. Further, no single theory of pionic nuclear binding has been able to reconcile all of the observations at all kinematics. As Miller concludes, this new data will present "an excellent opportunity to unravel a significant long-standing mystery involving the absence of nuclear pionic effects."

The proposed precision measurements of R will greatly aid the development of reliable global descriptions of existing inclusive electroproduction data on deuterium at moderate to high Q^2. This is critical for the extraction of the spin-dependent structure functions g_1 and g_2 from spin asymmetry measurements in the resonance region. The proposed measurements will allow a complete survey of the resonance region, and will permit an extraction of the Q^2 dependence of the L-T separated structure functions with very fine granularity in W^2 bins of (25 MeV)^2. Such models are necessary for accurate radiative correction calculations. Recently, both the CLAS [16] collaboration in Hall B and experiment E01-006 [17] in Hall C have completed electron spin asymmetry measurements utilizing ND3 targets. What was measured was the yield asymmetries for the scattering of beam electrons polarized both parallel and anti-parallel to the beam direction. For target polarizations both parallel and perpendicular to the beam direction, this yields the asymmetries $A_{||}$ and $A_{\perp}$, respectively. In Hall B it is possible to measure $A_{||}$ only, as perpendicular target fields are not feasible within the confines of the CLAS detector, while E01-006 was able to obtain both parallel and perpendicular target polarizations.

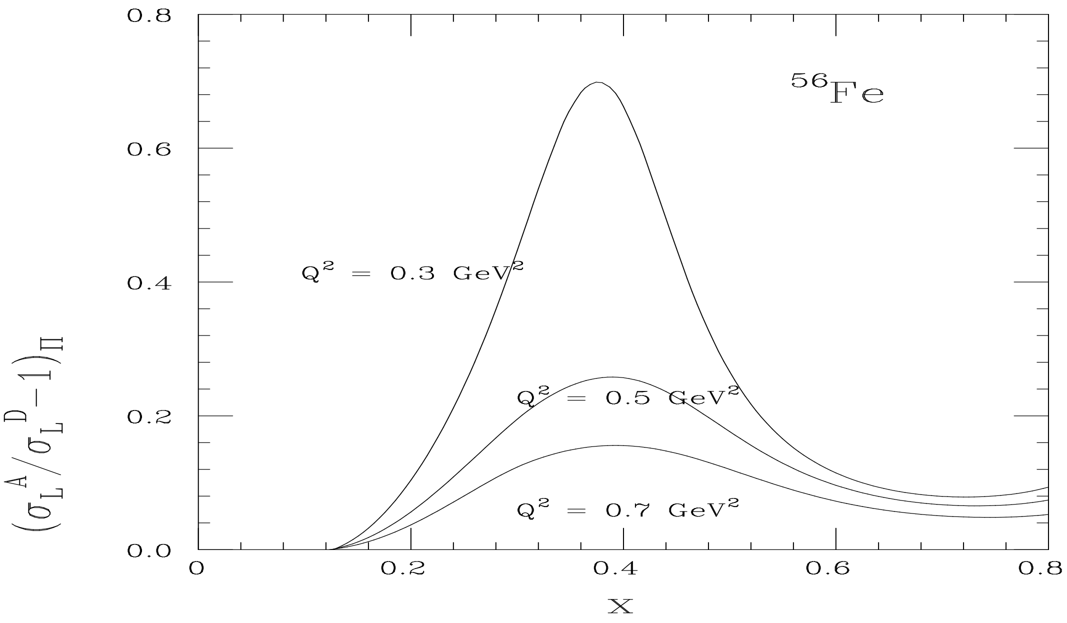

Figure 2: Plot from reference [8] showing the predicted sensitivity of inclusive longitudinal cross section in Iron to pion excess.

The photon helicity asymmetries, A_1 and A_2, can be determined from the electron asymmetries via

$$A_1 = \frac{C}{D}(A_{||} - dA_{\perp}), \tag{7}$$

and

$$A_2 = \frac{C}{D}(C^{'}A_{||} - d^{'}A_{\perp}). \tag{8}$$

The factors C, $C^{'}$, d, and $d^{'}$ are kinematic only, while the photon depolarization factor,

$$D = \frac{1 - \epsilon E^{'}/E)}{1 + \epsilon R}, \tag{9}$$

is a function of the unpolarized structure function ratio R. For $\epsilon R << 1$, the fractional uncertainty in $A_{1,2}$ coming from an uncertainty in R of δR is

$$\Delta A_{1,2}(\delta R) = \frac{\epsilon}{1 + \epsilon R} \approx \epsilon \delta R. \tag{10}$$

Using the World's previous proton average in the resonance region of $R = 0.06$ or a typical value from E94-110 of $R = 0.24$ leads to a difference of 9% in $A_{1,2}$ at $\epsilon = 0.5$. It is important to note that it is a linear combination of A_1 and A_2 that appears as the integrand in the generalized Gerasimov-Drell-Hearn (GDH) integral [13, 14, 15], to which the resonance region contributes the largest component at small Q^2.

We would like to stress that both experiments measure electron scattering *asymmetries*, and therefore, require a parameterization of the unpolarized structure functions in order to extract both $A_{1,2}$ and spin structure functions. For example, g_1 can be extracted via

$$g_1 = \frac{F_1(A_1 - \gamma A_2)}{(1+\gamma^2)} \propto F_1(1+\epsilon R) \propto \frac{F_2(1+\epsilon R)}{1+R}. \tag{11}$$

Therefore at $\epsilon \approx 1$ only knowledge of F_2 is needed for the extraction of g_1. It should be stressed that there has been no experiment in which the strength from F_2 and R have been separated for any significant portion of the resonance region. Hence, the relevant question becomes; how sensitive is the extraction of F_2 in the resonance region to different values of R? At typical JLab resonance region kinematics, the percent difference in F_2 extracted from cross section measurements assuming a value for R of either 0.2 or 0.0 varies from $\approx 2\%$ to $\approx 16\%$ [19].

3 Measurement of the Inclusive Cross Section

The inclusive scattering cross section will be determined by measuring the yield of scattered electrons which will be detected in the High Momentum Spectrometer (HMS) in Hall C. Measurement of the inclusive cross section for a range of ϵ values at fixed W^2 and Q^2 requires that the beam energy be varied. For each beam energy, and with the spectrometer at a fixed scattering angle, the spectrometer momentum will be varied such that W^2 is scanned from the elastic kinematics out though the resonance region and into the DIS region to $W^2 \approx 4.0$ GeV^2. Performing such scans at a variety of beam energies and scattering angles allows the entire resonance region to be surveyed in a range of Q^2 and ϵ values for each small W^2 bin. Examples of two such scans performed during E94-110 are presented in figure 3 as a function of W^2, and with a bin width of $\approx$ (25 MeV)^2. The statistical errors bars are included, but are typically smaller than the symbol size.

Each plot includes up to 5 individual momentum settings with a momentum bite of $+/-8\%$ in the HMS spectrometer. Adjacent runs overlap in the momentum bite by $\approx 3-4\%$. This allows a good check on the spectrometer momentum acceptance. After applying acceptance corrections, the agreement between overlapping bins from adjacent runs is typically within the statistical uncertainties. The cross section in overlapping bins has been averaged in the plots presented here. Also plotted is the fit to the E94-110 cross section data, denoted as 'Liang Model', as well as a fit to older SLAC data [18], denoted as 'H2 Model'.

4 Structure Function Extraction

The extraction of the structure functions from the cross section measurements will be accomplished in two complementary ways. First, Rosenbluth separations will be performed at each W^2, Q^2 where enough cross section measurements and range in ϵ exist to perform a good linear fit. Second, a global fitting procedure will be employed to separate the cross sections into longitudinal and transverse strength. Provided that enough

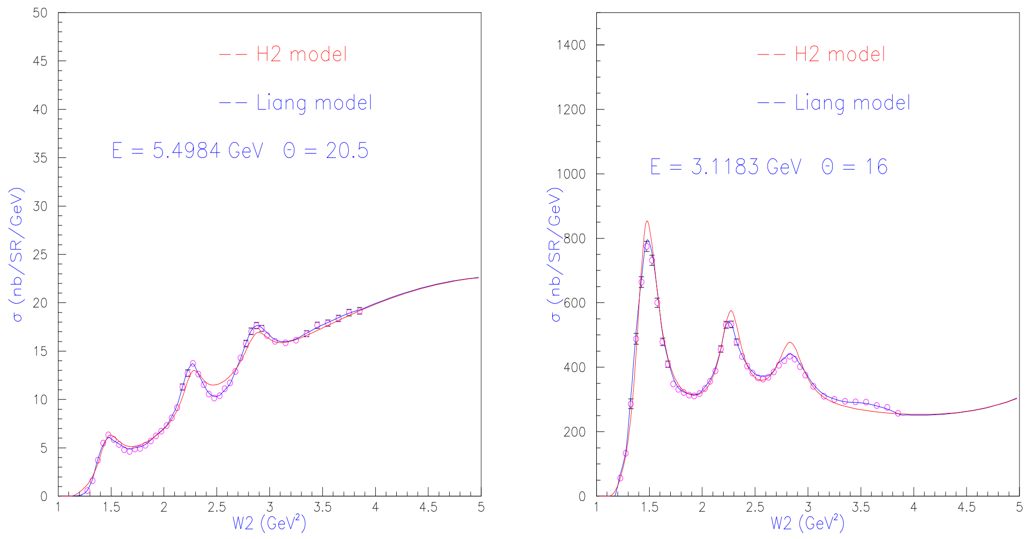

Figure 3: Cross sections measured in E94-110 at two different beam energies and scattering angles.

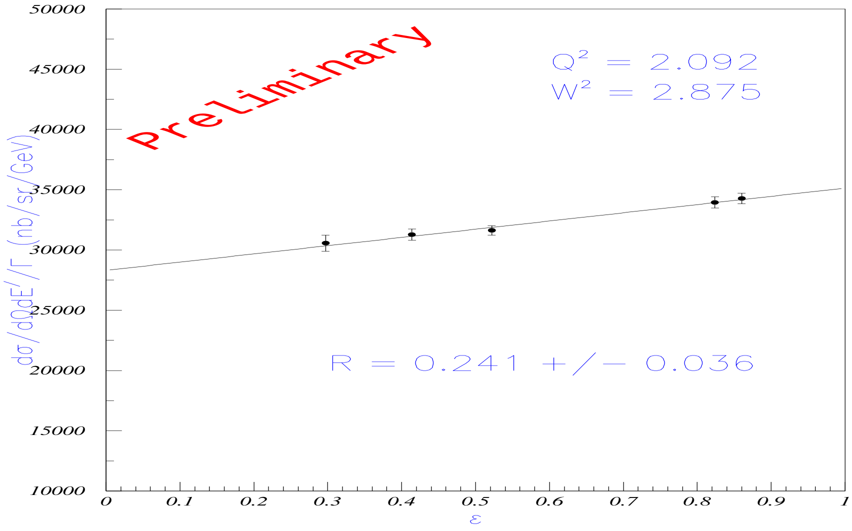

Figure 4: One of the 150+ Rosenbluth separations performed on the E94-110 data.

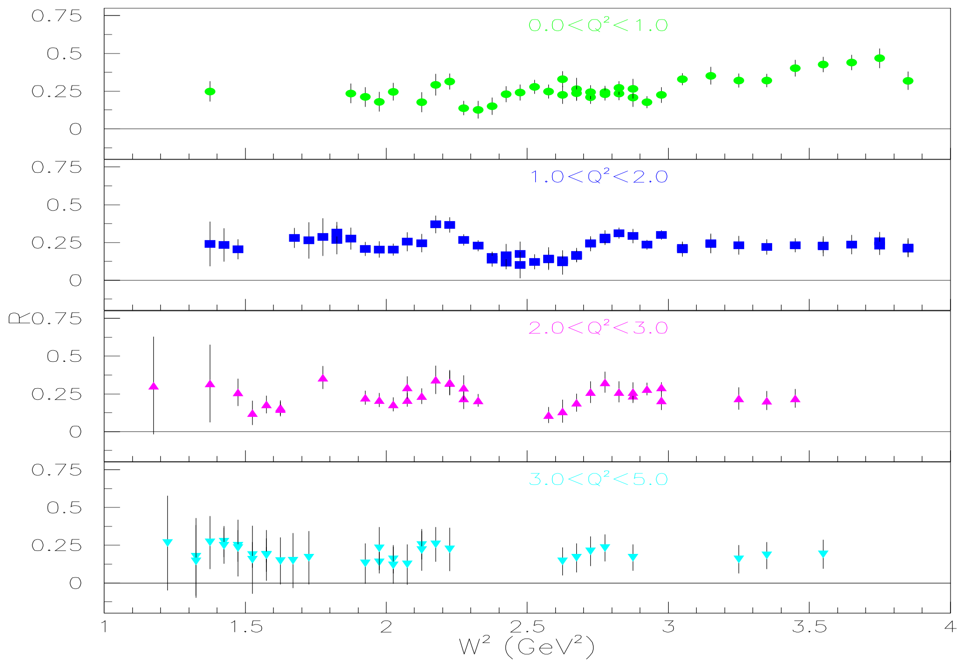

Figure 5: Rosenbluth extracted values of R as a function of W^2 for various Q^2 ranges .

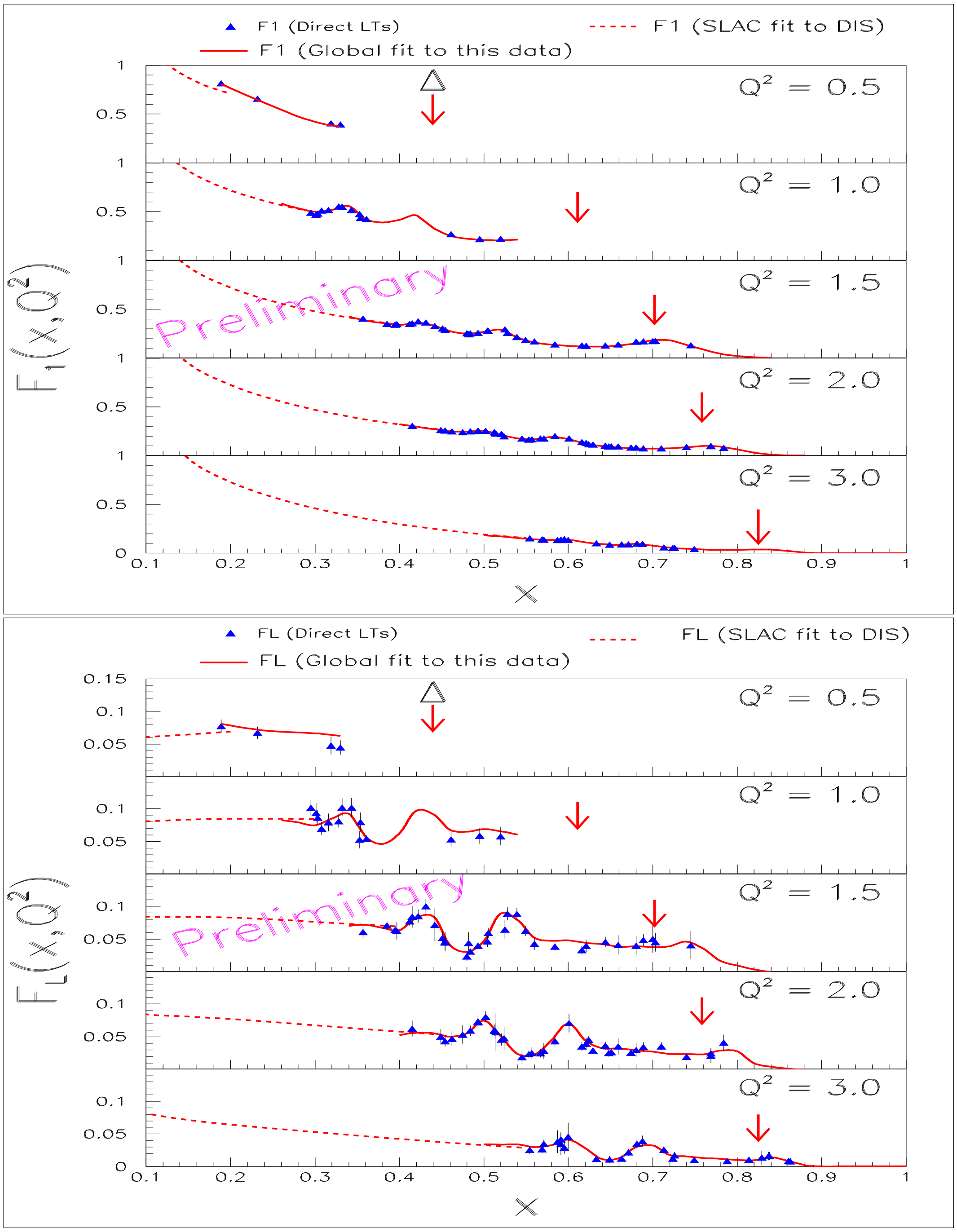

Figure 6: Rosenbluth extracted data for F_1 (top) and F_L (bottom). The triangles represent the data with full statistical and systematic error bars included. The solid curve is the result of the global fitting procedure, while the dashed curve is a fit to DIS data from SLAC.

of the kinematic space is covered, there is one unique way of doing this. An example of one of the 150+ Rosenbluth separations performed on the proton data is presented in figure 4 for the kinematics of the 3rd resonance peak and $Q^2 = 2.092$ (GeV/c)^2. Since the individual cross section measurements were taken at slightly different Q^2, the fit to the data was used to move all ϵ points to a common Q^2. Care was taken that this movement was small enough so that the uncertainty introduced was much smaller than the experimental point-to-point uncertainties.

A large subset of Rosenbluth separated R values extracted from the proton data are presented in figure 5 as a function of W^2 for various bins in Q^2. The same quality of data is expected for the proposed measurement and can be seen to be a vast improvement to the current World's data set when comparing to figure 1. Interestingly, R exhibits resonance behavior heretofore only observed in F_2. This resonance structure can also be seen in F_1 and F_L, which were extracted from the proton Rosenbluth separations and are presented in figure 6. Also plotted is the global fit, which is seen to be in excellent agreement with the Rosenbluth technique. A fit [10] of SLAC L-T separated DIS data is also shown and is seen to link smoothly to the resonance region data.

5 Systematic Uncertainties

At present, the world's best precision L-T separation measurements on deuterium have been performed by SLAC experiment E140X, to measure R in deep inelastic scattering. The point-to-point uncertainties for E140X are given in Table 1. The proposed experiment will be able to make resonance region measurements with a comparable level of precision. Much effort was put into both understanding and reducing the systematic uncertainties for E94-110. It is proposed that these same uncertainties will be achieved for this deuterium measurement. The point-to-point uncertainties for E94-100 are listed in Table 2. Also listed are the projected contributions to the cross section due to these uncertainties and the corresponding uncertainty in R extracted in the region of the Δ resonance.

5.1 Kinematics

The largest contribution to the point-to-point systematics comes from the uncertainties in the kinematics and is simply due to the large variation in the cross section with W^2 near the resonances. In order to help minimize these uncertainties, proton elastic scattering data will be taken at every beam energy and HMS angle setting, where possible. For elastic scattering, the difference of the reconstructed invariant mass, W, from the proton mass ($\Delta W = W$ - M_p) can be constructed and the dependence of ΔW on possible energy and angle systematics can be studied.

Experimental Quantity	Uncertainty	$\Delta\sigma(\%)$	ΔR
Beam Angle on Target	.05 mrad (.003^o)	0.1	0.005
Beam Energy	$1 \cdot 10^{-3}$	0.3	0.014
Scattered Electron Energy	0.05%	0.1	0.005
Target Density	0.2%	0.2	0.009
Scattering Angle	0.04 mrad (.002^o)	0.1	0.005
Beam Charge	$3 \cdot 10^{-3}$	0.3	0.014
Acceptance vs. θ	0.1%	0.1	0.005
Acceptance vs. p	0.1%	0.1	0.005
Detector Efficiency	0.1%	0.1	0.005
e^+/e^- background	0.1%	0.1	.005
Radiative Corrections	1.0%	1.0	0.000
	Total	1.1	0.039

Table 1: Published point-to-point systematic uncertainties from E140X

Experimental Quantity	Uncertainty	$\Delta\sigma(\%)$	ΔR
		Δ ($Q^2 = 1.0$)	Δ
Beam Energy	$4 \cdot 10^{-4}$	0.3	0.011
Scattered Electron Energy	$4 \cdot 10^{-4}$	0.2	0.007
Target Density	0.04%	0.05	0.002
Scattering Angle	0.2 mrad	0.4	0.015
Beam Charge	$1 \cdot 10^{-3}$	0.1	0.004
Acceptance	0.6%	0.6	0.022
Detector Efficiency	0.3%	0.3	0.011
Deadtime Corrections	0.1%	0.1	0.004
e^+/e^- Background	0.2%	0.2	0.007
Radiative Corrections	1.0%	1.0	0.040
	Total	1.35	0.052

Table 2: Point-to-point systematic uncertainties from the analysis of E94-110 and the corresponding uncertainty on R for the region of the Δ resonance at $Q^2 = 1$ (GeV/c)^2.

Fitting the ΔW dependence on systematic energy and angle offsets allows an extraction of these offsets. This procedure was used for the E94-110 data and yielded an uncertainty in the corrected beam energy of 0.04%, less than half that typically quoted from Hall C Arc measurements. The reconstructed W values for these data are plotted verses scattering energy in figure 5.1, for four different beam energies and twenty eight unique kinematic settings. It was found that the entire data set could be well described by assuming that the true HMS central angle was smaller than the nominal value by 1.3 mrad, and that the true HMS central energy was smaller than the nominal value by a constant fractional amount of -0.31%. The true beam energy was found to be smaller than the Arc measurements by an amount which varied with the energy. The reconstructed values for W are shown, both before (open symbols) and after (solid symbols) correcting for the kinematic offsets found from these studies. The corrected values are all seen to be within 1-2 MeV of the proton mass.

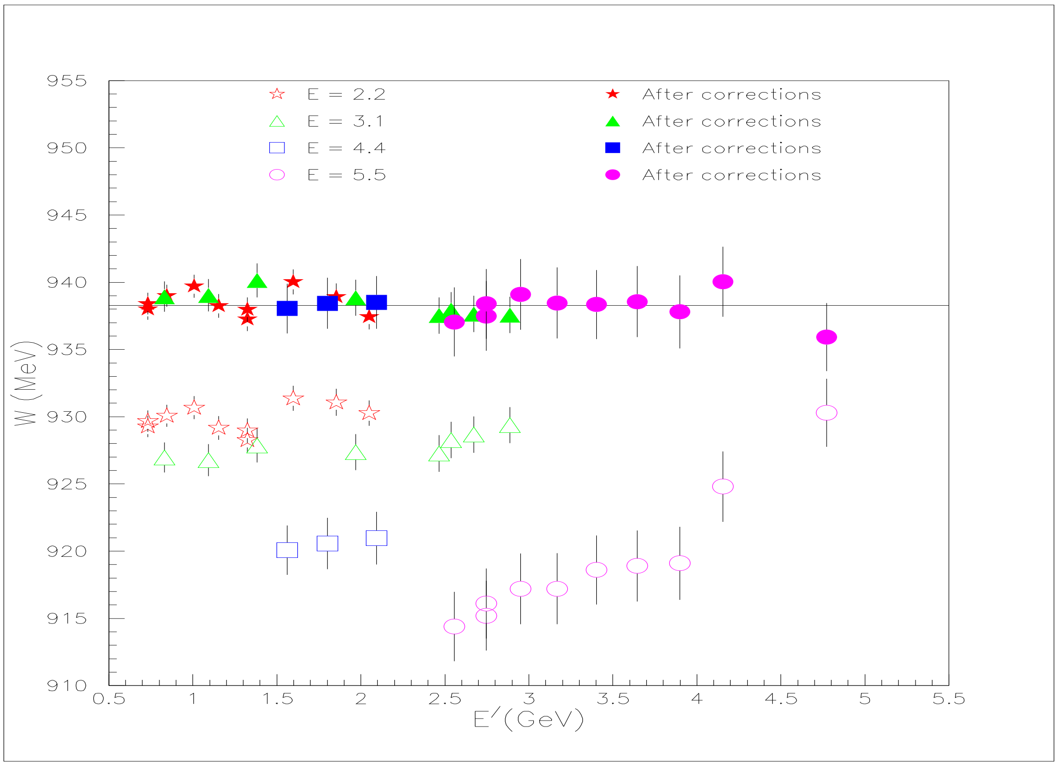

Figure 7: Reconstructed W vs. HMS momentum for elastic scattering kinematics. Open symbols represent data before kinematic corrections were applied, while the solid symbols represent the data after applying the kinematic corrections.

Accelerator cavity RF instabilities have been observed to cause variations in the beam energy on the order 0.05%. These variations of the beam energy can be measured using the BPMs (beam position monitors) in the Hall C Arc. These BPMs are read into the data stream every second and can be used to make relative beam energy corrections for the beam energy drift. Such corrections have been made by previous experiments and have resulted in the narrowing of missing mass peaks. Corrections for such beam energy variations were included in the proton analysis.

Just as the arc BPMs allow corrections for variations in beam energy to be made, information from the Hall C beamline BPMs allow corrections for beam position and angle on target to be made. In contrast to the arc BPMs, information from these BPMs are fed into the data stream on an event-by-event basis. Uncertainties in the beam position and angle on target directly translate into uncertainties in the reconstructed kinematics. We plan to use the Hall C fast raster with a spot size on target of ± 1 mm. Deviations in the vertical position of the beam will appear as a momentum offset in spectrometers. The effect of a beam position offset can be calculated from the optical matrix elements for the spectrometer. The first-order forward matrix elements for the HMS spectrometer are given in Table 3. The effect on the reconstructed momentum due to a 1 mm offset of the beam on target in the spectrometer dispersive direction (x_{tar}) is

$$\Delta P(1\text{ mm}) = \pm 0.1\text{ cm} \cdot (-3.0821) \cdot 0.27\ (\%/\text{cm}) = \pm 0.08\%, \tag{12}$$

where the reverse matrix element (≈ 0.27 %/cm) has been used to convert x'_{fp} to δ.

A study of the run-to-run beam steering stability was made during the running of E94-110. From this study, we measure run-to-run variations in x_{tar} of $\delta x_{tar} < .2$ mm. We use this as a worst case, and calculate a corresponding point-to-point uncertainty in in spectrometer momentum, P, of

$$\Delta P = \pm 0.2 \cdot \Delta P(1\text{mm}) = .024\% \tag{13}$$

The angle of the beam on target (x'_{tar}) enters as a direct uncertainty in the scattering angle if not corrected for. Again, the BPM information allows a correction to be made for this. The worst case point-to-point error is found to be the run-to-run x'_{tar} variations of $\Delta x'_{tar} \approx .04$ mrad.

HMS	x_{fp}	x'_{fp}	y_{fp}	y'_{fp}
x_{tar}	-3.0821	0.05681	0	0
x'_{tar}	0.1555	-.3273	0	0
y_{tar}	0	0	-2.2456	-2.569
y'_{tar}	0	0	1.4135	-.2836
δ	3.7044	-0.001688	0	0

Table 3: HMS $1st$-order forward matrix elements.

5.2 Target Density

The disadvantage of using a small raster size is an increase in localized target density fluctuation. Localized target density fluctuation, induced by an intense incident beam, can significantly modify the average density of a cryogenic target. Point-to-point uncertainties in the target density enter directly as point-to-point uncertainties in the total cross section and are current-dependent. The current-dependence can be measured by comparing the yields at fixed kinematics with varying beam currents. The deadtime-corrected yields should be proportional to the luminosity (and, therefore, the target density).

The result of such a 'luminosity scan' for E94-110 is shown in Figure 8, where the luminosity relative to that for zero current has been plotted on the vertical axis. The error bars on the data are statistical only and do not reflect fluctuations in the beam current. Assuming an error in the fit of $\pm 10\%$, due to systematic errors in the fit data and a run-to-run error in the current of $\pm 2\mu$A, the estimated point-to-point uncertainty in the target density is

$$\Delta\rho_t = 0.2 \cdot 0.1 \cdot 0.24\% = 0.05\%. \tag{14}$$

We propose to use a constant beam current of 80 μA for these measurements to reduce this uncertainty.

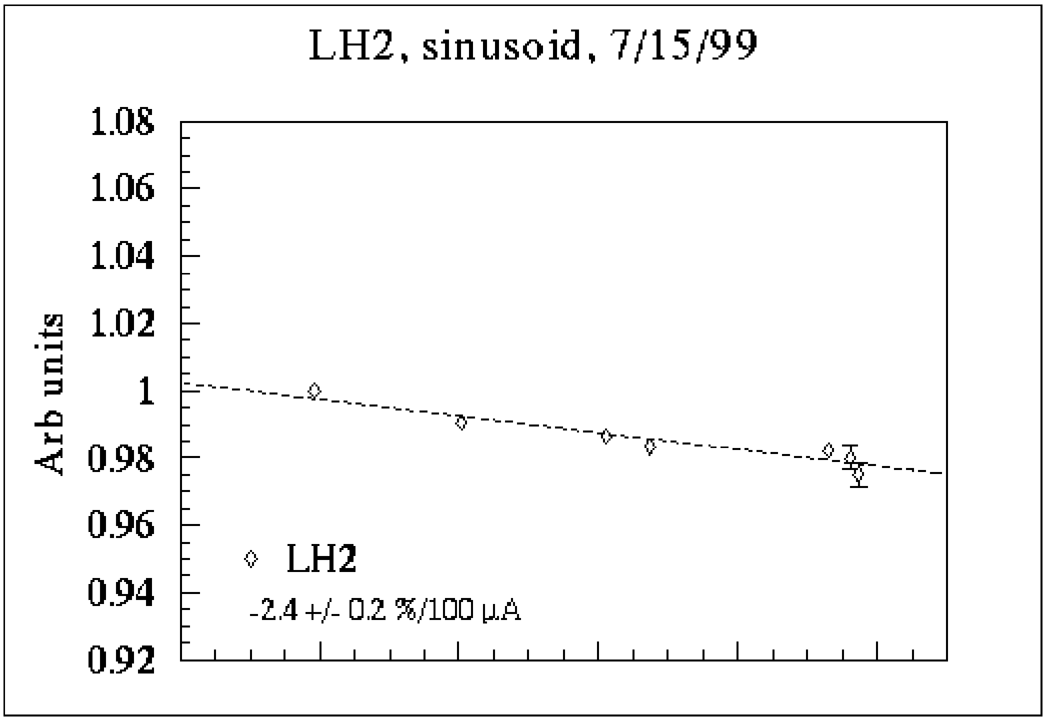

Figure 8: Luminosity scan data and fit taken 7/99. The range of the horizontal axis is 0 to 100 μA.

Other quantities which contribute to a systematic uncertainty in the total cross section are corrections for acceptance, detector efficiencies, and deadtime. All of these have been studied for E94-110 and a variety of other Hall C experiments and are believed to be well-understood. Reliable Monte Carlo models for both spectrometers exist, and have been shown to accurately reproduce the data for many different processes and kinematics. For the proton data, the model of the HMS was checked exhaustively and fine tuned to ensure the level of precision needed for high quality L-T separations.

5.3 Spectrometer Acceptance

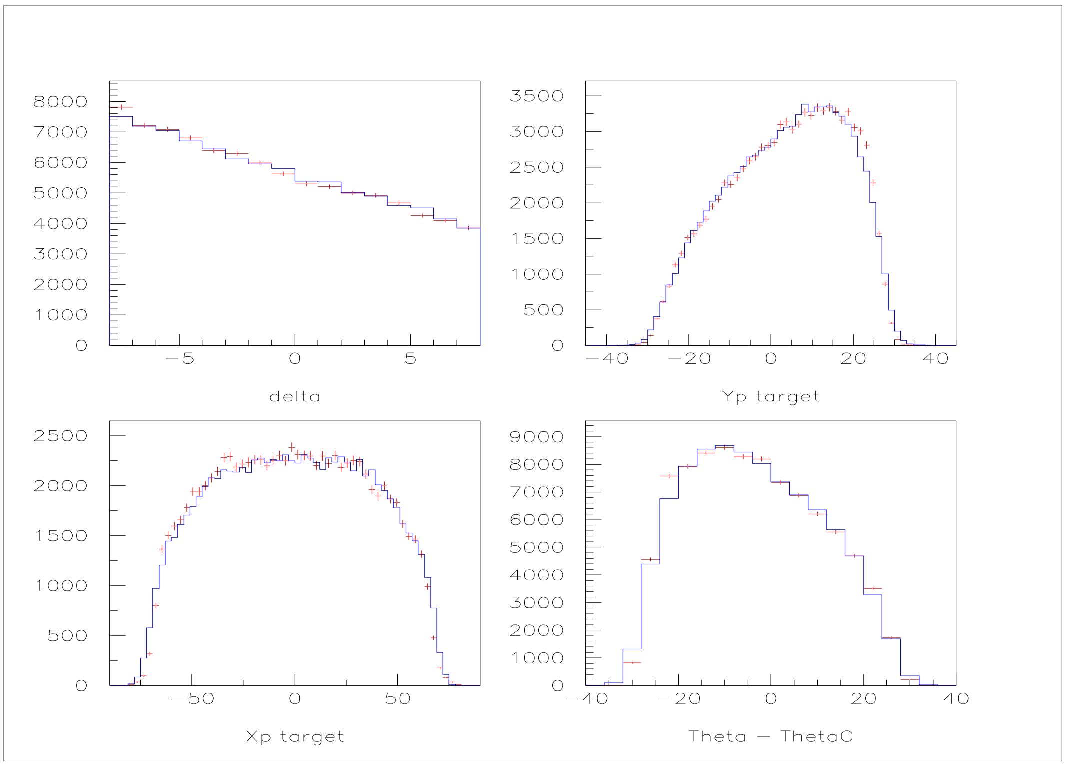

Figure 9: Comparison of the E94-110 data (red points with error bars) to the HMS Monte Carlo (blue histograms) for the reconstructed vertex quantities: δ (top left), $Y^{'}$ (top right), $X^{'}$ (bottom left), and $\theta - \theta_c$ (bottom right), which are described in the text. All angle units are in mrad.

A comparison of HMS Monte Carlo to E94-110 data for kinematics near the delta resonance is shown in figure 9. Comparisons of the distributions in δ, $Y^{'}$ (the in-plane scattering angle), $X^{'}$ (the out-of-plane scattering angle), and $d\theta$ (the difference of the full scattering angle from the central spectrometer angle) are shown, and the agreement is seen to be excellent. The point-to-point uncertainty in the acceptance corrections given in Table 2 has been estimated using this model of the HMS. For an extended target, there can be a relatively large difference in the acceptance for forward and backward angle scattering and is dominated by events being lost in the aperture defined by the second quadrapole magnet. Studies have been made of the effects on the acceptance due to shifts of various apertures within the uncertainty allowed by surveys of the spectrometer, as well as inaccuracies in the optics model. These studies indicate a combined point-to-point uncertainty on the acceptance and optics of 0.6%.

5.4 Detector Efficiencies

The efficiencies for the HMS shower and Cerenkov counters have previously been studied for inelastic (e,e') scattering [19]. Since the efficiency of the shower counter calorimeter increases with scattered electron energy, our worst case for the present experiment is for the kinematics in which the scattering is at high W and Q^2, and, therefore, low momenta. The uncertainties in the efficiencies for this case are $\pm 0.25\%$ for both the shower counter and Cerenkov counter. Studies of the tracking efficiencies have shown that once the rate dependence has been corrected for, the run-to-run variations are largely dominated by statistics. For the statistics expected, this uncertainty is estimated at 0.1%. The overall detector efficiency is estimated to be $\pm 0.3\%$

Proposed Kinematics

Table 4 lists the kinematics and cross sections we propose to measure, as well as a breakdown of beam time requirements. The differential cross sections for inclusive electron scattering will be measured according to the following definition:

$$\frac{d^2\sigma}{d\Omega dW^2} = \frac{\Delta N}{\Delta\Omega\Delta W^2}\frac{1}{Qnd}, \tag{15}$$

where ΔN is the counts per W^2 bin, n is the density of deuterium, d the target thickness, and Q is the integrated number of incident electrons on target. A minimum time of one half hour per kinematic setting, a maximum rate of 1000 Hz, and a beam current of 80 μA were used. The calculated rates listed are for bins of width $\Delta W^2 = (25\text{MeV})^2$ averaged over a momentum acceptance of $\pm 8\%$ and assuming an effective solid angle of the HMS of 6.5 msr at the Δ resonance. The data for the higher resonances comes in at higher rates and requires $\approx$ 50% additional beam time. The data acquisition time listed in Table 4 reflects the total time required for the Δ resonance only. The SOS will be used to collect positron yields (from neutral pion production) for charge symmetric background studies and will be run in a simultaneous single arm mode with the HMS data and, so, this adds little time to the beam time request. The extraction of neutron structure functions requires the subtraction of the proton data taken in E94-110. As a cross check on relative normalizations, we propose to do measurements of the hydrogen resonance region cross sections for $Q^2 < 3.0$ (GeV/c^2)^2 to compare to E94-110. This will require an additional 16 hrs. A minimum central spectrometer momentum setting of 400 MeV/c was assumed. All proposed measurements will use the Hall C 4 cm deuterium target. In addition, elastic proton data will be taken at all angles and energies for kinematic uncertainty checks.

The chosen beam energies in the table assume a linac energy of 1.12 GeV (1.16, 2.28, 3.24, 4.52, 5.64), with the exception of two beam energies which assume a linac energy of 0.80 GeV (1.64, 4.04). Both base energies are standard CEBAF accelerator tunes.

The required beam time was determined such that the statistical accuracy per W^2 bin was $\approx$ 3 times greater than the systematic point-to-point accuracy expected. The rates were estimated based upon a fit of previous deuterium resonance region cross section data from JLAB [19].

Q^2_Δ $(GeV/c)^2$	E (GeV)	E'_Δ (GeV)	θ_Δ (deg)	ϵ_Δ	$Rate_\Delta$ (Hz)	Time (Hours)
0.5	1.16	0.55	52*	0.54	1 K	0.5
	1.64	1.0	33	0.78	1 K	0.5
	4.04	3.4	11	0.97	1 K	0.5
1.0	1.64	0.77	52*	0.53	1 K	0.5
	2.28	1.4	33	0.77	1 K	0.5
	4.52	3.6	14	0.95	1 K	0.5
2.0	2.28	0.87	60*	0.43	65	0.5
	3.24	1.8	35	0.73	285	0.5
	5.64	4.2	17	0.92	1 K	0.5
3.0	3.24	1.3	52*	0.51	16	2
	4.04	2.1	35*	0.70	40	1
	5.64	3.7	22	0.86	172	0.5
4.0	3.24	0.77	79*	0.23	1	22
	4.04	1.6	47*	0.51	3	8
	5.64	3.2	27	0.77	53	1
5.0	4.04	1.0	66*	0.29	1	22
	4.52	1.4	52*	0.42	3	8
	5.64	2.5	35	0.66	6	4
						Total **73**

Table 4: Beam time requirements for all proposed measurements. All kinematics and rates shown are for a single bin in W^2 of 25 $(\mathrm{MeV})^2$ width at the Δ resonance. Positron data will be taken in the SOS for the angles indicated by an asterisk.

The beam time requested for this experiment is listed in Table 5. The total data acquisition time listed reflects the total time from Table 4, as well as an additional 40 hours to complete the higher resonances. We also require 60 hours for dummy target runs which are needed to subtract the yield contributions from the aluminum end caps of the target, 24 hours to complete the hydrogen elastic scattering measurements, and 16 hours to obtain the hydrogen resonance region data which is needed to cross check with E94-110. The beam time requested for the dummy target will provide adequate statistics for extracting L-T separated cross sections for aluminum. Also, since the positron data comes in at a slower rate, we request an additional 22 hours to complete these measurements. We assume one-quarter hour for each angle change required at a given beam energy, and one-quarter hour for each spectrometer central momentum change not possible to be done concurrently with angle changes. Combined with one day for checkout, we request a total beam time of 13 days.

	Time Required (Hours)
Data acquisition (Deuterium Δ)	73
Data acquisition (Deuterium $W^2 > \Delta$)	40
Data acquisition (Dummy)	60
Data acquisition (hydrogen elastics)	24
Data acquisition (hydrogen resonance region)	16
Data acquisition (additional positrons)	22
Angle changes (12)	3
Spectrometer momentum changes (60)	15
Major beam energy changes (1)	8
Minor beam energy changes (5)	20
Checkout	24
Total	**305**

Table 5: Breakdown and tabulation of the total time requested. Based on previous experience, we assume one-half hour for angle changes, 15 minutes for momentum changes, eight hours for linac energy changes (major), and four hours for each energy change accomplished by changing the number of cycles (minor).

The Collaboration

The collaboration consists of people who have participated in a substantial amount of Hall C running. The collaboration has implemented and proven successful techniques to reduce systematical uncertainties in Hall C experiments, including detailed studies of spectrometer optics, spectrometer survey studies, raster phase analysis, and additional beam line instrumentation. This collaboration has the on-site experience, knowledge and expertise requisite to perform a precision measurement of the type proposed.

Conclusion

Using the existing Hall C apparatus, we propose to perform a global survey of L-T separated unpolarized structure functions on deuterium throughout the nucleon resonance region with an order of magnitude better precision than has been achieved before. The recent analysis of the proton data from E94-110 clearly show that these goals are both realistic and attainable.

REFERENCES

1. JLAB experiment 94-110, C.E. Keppel spokesperson
2. Phys. Rev. D64, 054004 (2001)
3. W. Melnitchouk,Nucl. Phys. A699, 278 (2002)
4. P. Eden *etal*. JHEP110 40,2001
5. S. Jeschonnek, hep-ph/0201113
6. S. Liuti, hep-ph/0111063
7. F.E. Close and N. Isgur, Phys.Lett. B509, 81 (2001)
8. J. Miller, Phys.Rev. C 64, (2001)
9. M.N. Rosenbluth, Phys. Rev. 79, 615 (1956)
10. L.W. Whitlow et al., Phys. Lett. B250, 193 (1990)
11. S. Dasu et al., Phys. Rev. Lett. 61, 1061 (1988)
12. L.H. Tao, Ph.D. Thesis, The American University (1994)
13. S.B. Gerasimov, Sov. J. Nucl. Phys. 2, 430 (1966)
14. S.D. Drell and A. C. Hearn,Phys. Rev. Lett. 16,908 (1966)
15. X. Ji, C. Kao and J. Osborne, Phys. Lett. B 472, 1 (2000)
16. JLAB experiment E93-009, S.E. Kuhn spokesperson
17. JLAB experiment E01-006, O. Rondan spokesperson
18. C.E. Keppel, Ph.D. Thesis, The American University (1994)
19. I. Niculescu. Ph.D. Thesis, Hampton University (1999)